Lawrence Berkeley Laboratory
UNIVERSITY OF CALIFORNIA

Submitted to Nuclear Physics

QUANTAL DYNAMICS OF CHARGE EQUILIBRATION IN DAMPED NUCLEAR COLLISIONS

E. S. Hernandez, W. D. Myers, J. Randrup and B. Remaud

October 1979

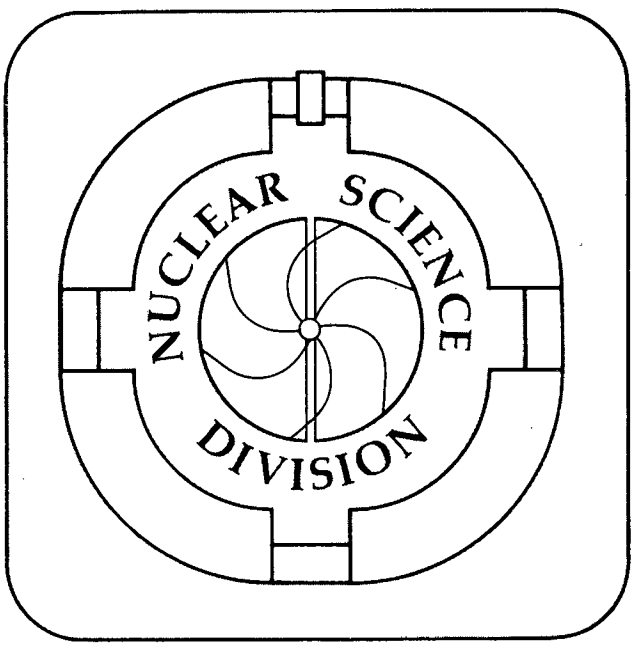

Prepared for the U.S. Department of Energy under Contract W-7405-ENG-48

DISCLAIMER

QUANTAL DYNAMICS OF CHARGE EQUILIBRATION IN DAMPED NUCLEAR COLLISIONS*

E. S. Hernandez,** W. D. Myers, J. Randrup and B. Remaud†

Nuclear Science Division
Lawrence Berkeley Laboratory
University of California
Berkeley, CA 94720

Abstract

The change in the projectile charge and the dispersion in its value that arise in the course of a damped nuclear collision are treated quantum mechanically in terms of a collective mode analogous to the Giant Dipole Resonance in spherical nuclei. First a classical trajectory calculation is performed to determine the time evolution of the neck which opens between the two nuclei during the reaction and a simplified hydrodynamic model is used to estimate the corresponding values of the inertial and damping coefficients for the charge asymmetry degree of freedom. Then a damped time-dependent Schrödinger equation is solved for the final values of the mean charge $\langle Z \rangle$ and its dispersion Γ_{FWHM} and these predictions are compared with measured values.

---

*This work was supported in part by the U. S. Department of Energy under Contract W-7405-ENG-48.

**Permanent address: Departamento de Fisica, Facultad de Ciencias Exactas y Naturales, 1428 Buenos Aires, Argentina.

†Permanent address: Institut de Physique, Université de Nantes, 2 rue de la Houssinière, 44072 Nantes, France.

1. Introduction

In quasi-elastic and deep-inelastic nuclear reactions charge equilibration appears to occur quite rapidly. Even when the collision involves relatively little energy loss or net mass transfer the charge-to-mass ratio of the projectile-like fragment is observed to have shifted to an equilibrium value close to that of the composite system. This rapid movement of protons in one direction and neutrons in the other can be viewed as a collective mode associated with isovector-type hydrodynamical flow in the dinucleus analogous to the Steinwedel-Jensen[1]) description of the Giant Dipole Resonance in ordinary nuclei. Since we find that the characteristic energy of such a mode is typically much larger than the nuclear temperatures encountered, the fluctuations in the charge asymmetry degree of freedom are expected to come mainly from zero-point motion. Insofar as it is appropriate to associate such a collective coordinate with the charge on the projectile-like fragment, we expect that the width of the measured charge distribution will be dominated by quantal (rather than statistical) effects.

In nuclear fission the widths of the change distributions observed have been associated by Fong (see ref. [2])) with statistical fluctuations due to the internal excitation of the nucleus. However, Hill and Wheeler pointed out that in a hydrodynamical description fluctuations in the division of charge are to be expected from quantum mechanical zero-point motion even when there is no excitation

energy[3]). Such a description of the charge asymmetry mode has already been applied with some success by Swiatecki and Blann to charge and mass distributions seen in fission[4]), and more recently to heavy-ion reactions by Moretto[5]), by Berlanger et al.[6]), and by Hofmann,, Gregóire, Lucas and Ngô[7,8]). However, as pointed out by Nifenecker et al.[9]), it is essential to consider the time dependence of the shape of the system in order to correctly establish the connection between the GDR-like collective motion and the width of the charge distribution which is experimentally observed.

Roughly speaking, the inertia associated with the charge asymmetry degree of freedom is inversely proportional to the size of the neck connecting the two colliding nuclei. Consequently, the charge dispersion associated with zero-point motion in this degree of freedom would go to zero if the pinch-off of the neck during the final stage of the collision were to take place adiabatically. In actual fact, trajectory calculations[10]) predict that the pinch-off takes place sufficiently rapidly that the width of the charge distribution is "frozen in" by the increasing inertia. In order to make a quantative estimate of these non-adiabatic effects we have undertaken to solve the time-dependent Schrödinger equation for a simple dynamical model of the charge asymmetry degree of freedom.

In the next section we describe the geometrical, hydrodynamical model that we have used to calculate the time dependence of the stiffness, inertia and damping for this GDR-like isovector mode during a nuclear collision. In the third section we describe the time-dependent Schrödinger equation calculations that serve to connect the

initial state of the system to the final charge distributions that are measured. In the fourth section these calculations are compared with experiment and in the final section we discuss the results and consider briefly other approaches towards describing the same phenomena.

2. Description of the model

The mass asymmetry of the dinuclear complex can be specified by the mass number A of the projectile-like binary partner. In order to describe the division of charge between the two partners, for a given mass asymmetry, we use the isospin component of the projectile-like nucleus $T = \frac{1}{2}(N-Z)$. The potential-energy surface of the dinucleus varies rather gently in the A-direction while the strong symmetry energy makes it much steeper in the T-direction. Furthermore, the dynamical evolution along the mass asymmetry proceeds relatively slowly and can often be entirely neglected. It is therefore sensible to discuss the dynamics of the charge asymmetry coordinate T for a fixed value of the mass asymmetry.

2.1 Dynamics of the dinucleus

In describing the overall dynamics of the dinucleus we adopt the model developed in refs. [10,11]), for which a brief summary is given below.

The dinuclear complex is depicted as illustrated in fig. 1: two spherical nuclei of mass numbers A and B joined by a small cylindrical neck. The mass and charge numbers A and Z refer to the projectile-like partner. The equivalent sharp radius is given by the following fit to the Droplet Model prediction[12]),

$$R_A = 1.28\, A^{1/3} - 0.76 + 0.8\, A^{-1/3} \quad . \tag{1}$$

The corresponding central radius which locates the nuclear surface profile is related to R_A by

$$C_A = R_A - b^2/R_A \tag{2}$$

where b = 1 fm is the nuclear surface diffuseness[13]).

The smallest distance between the two spherical nuclei is then given by

$$s = R - C_A - C_B \quad , \tag{3}$$

where R is the separation between the two nuclear centers. Furthermore, the radius of the neck is denoted by c and its length d is taken from the approximate expression

$$d \approx s + \frac{c^2}{2\bar{R}} \quad , \tag{4}$$

where the "reduced" radius $\bar{R}$ is given by

$$\bar{R} = \frac{C_A C_B}{C_A + C_B} \tag{5}$$

The potential energy of the dinucleus has the form

$$V = V_A + V_B + V_C + V_{AB} \quad , \tag{6}$$

where V_A and V_B denote the energies of the two individual spherical nuclei having mass numbers A and B, as given by the Lysekil mass formula[14]). Furthermore, V_C is the electrical potential between the

spheres; it is approximated by the Coulomb potential when the two spheres do not intersect ($s \geqslant 0$) and by a linear potential otherwise ($s \leqslant 0$). The remaining energy V_{AB} is associated with the interaction zone. Following a suggestion by Swiatecki[15], as modified in ref.[11], we use

$$V_{AB} = 2\pi c(d_{eff}-c) + 4\pi \bar{R}b\Phi\left(\frac{d}{b}\right)e^{-c^2/2\bar{R}b} \tag{7}$$

Here $d_{eff} = d - s_{crit}(1 - c/2\bar{R})$ is an effective neck length which takes account of the nuclear surface diffuseness [15]; we use $s_{crit} = -\Phi(0) \approx 1.78$ fm. The first term in the above expression is the surface energy associated with the cylindrical neck. The electrical energy is neglected. The second term represents the additional proximity energy arising from the nuclear interactions of the two surfaces facing each other (see Blocki et al.,[12]); the exponential factor represents a rough attempt to reduce this contribution when the two surfaces form an angle with one another.

The dinuclear motion is subject to the friction generated by the one-body dissipation mechanism[16]. The transfer of nucleons between the two nuclides produces a friction force acting on the relative motion of the two spheres. Their inertias are calculated under the assumption of rigid spheres. Furthermore, the motion of the neck radius c is counteracted by the wall dissipation in the cylinder,

$$F_c^{diss} = -\frac{1}{2}\frac{\partial}{\partial \dot{c}}(\rho \bar{v} 2\pi c d\, \dot{c}^2\, e^{-d/(b+c)}) \tag{8}$$

The exponential factor is included so as to diminish the dissipation for a long narrow neck, as is suggested by the general theory of one-body dissipation[17]). The balancing of this dissipative force with the conservative force implied by the potential energy described above determines the instantaneous rate of change in the neck radius.

Apart from the moderate arbitrariness with respect to the details of the neck dynamics, the model contains no adjustable elements. It has been shown to give a reasonable reproduction of the average trends in the experimental data on damped collisions[11]), and we believe that it provides the presently best available estimation of the temporal evolution of the neck.

At the present stage of development of our approach to describing charge equilibration we have used the results of the trajectory calculation as input to the calculation of the dynamical evolution of the charge asymmetry. The next logical step in this program would be to consider the coupling of the charge asymmetry to the other dynamical variables by simultaneous solution of the corresponding coupled equations of motion. For target and projectile systems with large differences in Z/A, such coupling may give rise to the prediction of observable changes in energy and angular distributions caused by the initial surge of particles through the neck as it opens up.

Typical results obtained from the trajectory calculations described above are shown in fig. 2a. The time evolution of the neck radius c and the neck length d is plotted for the case of 430 MeV

^{86}Kr on ^{72}Mo, at an impact parameter corresponding to an angular momentum of 60$\hbar$. Rather than the cylinder radius c, the figure displays a slightly larger effective neck radius defined by

$$c_{eff}^2 = c^2 + 2\,\bar{R}b\Phi\left(\frac{d}{b}\right)e^{-c^2/2\bar{R}b} \tag{9}$$

This quantity is considered because of the possibility of some exchange between the two nuclei before the neck is established or between the two juxtaposed surfaces outside the neck[18]). Because of this proximity contribution, the displayed neck radius does not rise vertically when the two nuclei come within the critical separation where the neck is established. No similar rounding off of the curve can be seen at the end of the collision because the nuclei are further apart when the cylinder radius drops to zero and the proximity contribution is negligible. The general appearance of $c_{eff}(t)$ is a rapid growth in the early part of the collision, mostly reflecting the forced geometrical overlap of the two spheres, followed by a gently sloping plateau as the two nuclei move apart again, finally to be terminated by a rather sudden collapse.

The corresponding behavior of the neck length d is an initial rather constant value of $d \approx s_{crit}$ associated with the frozen geometrical overlap of the two nuclei. As the nuclei move apart the neck length grows until the collapse occurs. Before contact and after pinch-off the value of the neck length shown in the figure (equal to the surface separation s) has no physical significance.

Under the figure the five small drawings show the appearance of the dinucleus at various stages of the collision.

In this figure, and throughout, the time is measured in units of 10^{-22} sec which is a convenient unit for nuclear physics problems; following the suggestion by Alonso[19]) we denote this time unit as dsec.

2.2 The charge asymmetry mode

Once the time evolution of the dinuclear geometry has been determined from the trajectory calculation, the dynamical coefficients for the charge asymmetry mode can be calculated. For the stiffness a conventional nuclear mass formula is used, and for the inertia and damping a rather simplified hydrodynamical model is employed.

2.2a The driving potential

The potential energy, considered as a function of the charge asymmetry coordinate T, is of the harmonic form

$$V(T) = \text{constant} + \frac{1}{2}K(T-T_o) \tag{10}$$

For two nuclei with mass numbers A and B the stiffness K and the equilibrium value T_o are given by

$$K = 8\kappa a_1\left[\frac{1}{A} + \frac{1}{B}\right] - 8\kappa a_2\left[\frac{1}{A^{4/3}} + \frac{1}{B^{4/3}}\right]$$

$$+ 2c_3\left[\frac{1}{A^{1/3}} + \frac{1}{B^{1/3}}\right] - \frac{2e^2}{R} \quad , \tag{11}$$

and

$$T_o = \frac{A}{2} + \left\{ 4\kappa a_2 \left(\frac{1}{A^{1/3}} - \frac{1}{B^{1/3}} \right) - \left[8\kappa \left(\frac{a_1}{B} - \frac{a_2}{B^{4/3}} \right) + \frac{2c_3}{B^{1/3}} - \frac{e^2}{R} \right] (Z_A + Z_B) \right\} / K \qquad (12)$$

when using the same macroscopic mass formula as employed in the trajectory calculations[14]). (The use of a more modern mass expression such as the Droplet Model leads to about the same result[20]). The various coefficients are,

$$\begin{aligned} a_1 &= 15.4941 \text{ MeV}, \\ a_2 &= 17.9439 \text{ MeV}, \\ \kappa &= 1.7826, \\ c_3 &= 0.7053 \text{ MeV}, \\ e^2 &= 1.44 \text{ MeV fm}. \end{aligned} \qquad (13)$$

We wish to point out that the equilibrium value of T_o does <u>not</u> correspond to having the same charge-to-mass ratio in the two nuclei. Generally the total energy is minimized when the charge-to-mass ratio is larger in the smaller of the two nuclei. This is true when the two nuclei are well separated, and remains true to some extent when they are in contact.

The stiffness coefficient K depends on the separation R but this dependence is rather weak in the interesting range of separations. The oscillator has therefore a nearly constant stiffness as a function of time.

2.2b The inertia

In the present investigation, where we consider the charge asymmetry to be an elementary collective mode in the dinucleus, the kinetic energy can be written

$$E_{kin} = \frac{1}{2} M\dot{T}^2 \quad , \tag{14}$$

where M is the inertial mass parameter associated with T. To estimate this quantity we consider the hydrodynamical flow of the proton and neutron fluids through the neck.

The inertial mass corresponding to uniform flow through a cylindrical neck is given approximately by

$$M_{cyl} = \frac{4m^*d}{\pi c^2 \rho_o} \quad . \tag{15}$$

Here $\rho_o = 0.145$ fm^{-3} is the standard nuclear density. For the effective mass we use the value $m^* = 0.7m$, which studies of the Giant Dipole Resonance have shown to be appropriate for describing the inertial properties of isovector flows in nuclei[21,22]). The additional contribution to the inertia from the flow field within the nuclei at each end of the neck is roughly approximated by assuming that the neck flow extends into the nuclei at each end by a distance equal to the neck radius, so that the effective length of the neck becomes (d + 2c). Alternatively, we might have used the inertia associated with non-viscous flow through a circular hole in a thin wall in nuclear matter that is given by[23,24])

$$M_{bulk} = \frac{2m^*}{c\rho_o} \quad , \tag{16}$$

and to lowest order in $(c/\bar{R})$ this value can be taken for the inertia associated with the flow inside the two nuclei at each end of the cylindrical neck. (In the above two expressions we have set to unity the factor $A^2/4NZ$ which arises from the fact that the density of protons is somewhat smaller than the density of neutrons so that the proton fluid must move faster than the neutron fluid. This is accurate to within a few percent.)

In the actual calculations we wish to use a hydrodynamic viscocity to estimate the damping of the charge asymmetry mode. For the cylinder the viscous flow profile is parabolic rather than constant, giving rise to an inertia which is increased by 4/3 over the irrotational value. Even though this is an almost meaningless refinement considering how crudely we have approximated the flow fields within the dinuclear complex, we shall assume that the same scale factor applies and the final expression used for the inertia is then

$$M = \frac{4}{3} \frac{4m^*}{\pi c^2 \rho_o} (d + 2c) \tag{17}$$

2.2c The damping

The damping of the charge asymmetry mode has been estimated by using the same value of the hydrodynamical viscosity that is required to reproduce the observed width of the Giant Dipole Resonance in spherical nuclei. The procedure serves merely to approximately fix the magnitude of the damping.

Thus, for viscous flow through a cylinder the kinetic energy per unit length is

$$E_{kin} = (\pi \rho_o p^2 c^6)/(96 \eta^2 d) \quad , \tag{18}$$

where p is the pressure difference and η is the viscosity coefficient[23]). The rate of energy loss per unit length is

$$\dot{E}_{kin} = -(\pi \rho^2 c^4)/(8 \eta d) \quad . \tag{19}$$

Consequently, the friction coefficient γ entering in the equation of motion for the charge asymmetry is given by

$$\gamma = -\dot{E}_{kin}/2E_{kin} = 6\nu/c^2 \tag{20}$$

where $\nu = \eta/\rho_o$ is the kinematic viscosity. In order to reproduce the width of the Giant Dipole Resonance in spherical nuclei this quantity should have the value[25])

$$\eta = 1.35 \text{ fm}^2 \text{ dsec}^{-1} \quad . \tag{21}$$

The friction coefficient is then taken to be

$$\gamma = (8.10/c^2) \text{ dsec}^{-1} \tag{22}$$

Once the quantities K, M and γ have been expressed in terms of the geometrical properties of the system (c, d and R) their time-dependence can be estimated in a number of ways. We have chosen to use the classical trajectory calculations described above because they were readily available and were known to give a reasonable description of other aspects of the collision process.

In part (b) of fig. 2 the reciprocal of our simplified hydrodynamical estimate for the value of the mass parameter M, from eq. (17), is plotted against time for three different impact parameters. For the most grazing collision shown here, corresponding an orbital angular momentum of 108$\hbar$, the period of oscillation in the charge degree of freedom is never less than 12 dsec and the motion is heavily damped. Consequently, the charge equilibration (which is discussed in greater detail in connection with fig. 3) is barely able to take place. For the more central collisions, for which the period is smaller and the damping less, complete equilibration takes place before the neck pinches off. For these longer lasting collisions where the period of the oscillations is about 8 dsec the gradual increase in the mass parameter M (gradual decrease of 1/M in the figure) takes place almost adiabatically. Consequently, we find in the quantal calculations described in the next section, that the zero point width in this degree of freedom decreases smoothly with time until it is frozen in by the abrupt increase in mass M and damping γ at the end of the collision.

3. Quantal treatment of a time-dependent damped oscillator

The model presented in the preceding chapter describes a particle with time-dependent mass M(t), from eq. (17), placed in a harmonic oscillator field with stiffness K(t), from eq. (11), and centered at the position $X_o(t)$. The corresponding (undamped) Hamiltonian can then be written as

$$H_o(t) = \frac{1}{2M(t)} p^2 + \frac{1}{2} K(t) (x - X_o(t))^2 \qquad (23)$$

From the dynamical trajectory calculations discussed in Section 2, we can extract a typical frequency $\Omega = \sqrt{K/M}$ for this harmonic oscillator. This value, along with the corresponding typical values of the inertia M, stiffness K, phonon energy $\hbar\Omega$ and friction parameter γ, are displayed in table 1 for both dinuclear systems $^{86}Kr + ^{92}Mo$ and $^{132}Xe + ^{197}Au$. These quantities have been selected at the point of maximum neck opening along the head-on trajectories. We recognize that in both cases the phonon energy is substantially larger than the expected temperature τ reached in ordinary damped nuclear collisions. Therefore one needs to treat the mode quantally rather than classically. Since ordinarily $\hbar\Omega$ is several times larger than τ we shall in fact assume that the thermal fluctuations arising from the coupling of the oscillator to the rest of the system are neglible; it then suffices to follow the evolution of only a single wave function throughout the equilibration process.

As discussed in the preceding section, the charge asymmetry mode is expected to be damped. It is therefore necessary to make room for

dissipation in the quantal treatment of the mode. Dissipation in quantum mechanics constitutes a non-trivial problem which has received much attention for several decades (see e.g., ref. [26]) for a survey). Recently, a discussion has been given of the motion of a Gaussian wave packet in a general time-dependent harmonic field, in the presence of a loss mechanism[27]). Following this work we shall adopt the frictional Schrödinger equation of Kostin[28]) and Kan and Griffin[29]).

$$i\hbar\dot{\psi} = (H_o + W)\,\psi \quad , \tag{24}$$

in our present investigation. The non-linear frictional term can be written

$$W = \hbar\gamma(t)(S - \langle S\rangle) \quad , \tag{25}$$

where $\gamma(t)$ is the time-dependent friction coefficient of the oscillator and S is the phase of the wave function, $\psi = |\psi|e^{iS}$; the average of S is with respect to the instantaneous wave function $\psi(t)$.

It has been shown that the following Gaussian wave function is a solution of the above frictional Schrödinger equation[26]):

$$\psi(x,t) = (2\pi)^{-1/4}\left(\frac{1}{\alpha} + \frac{1}{\alpha^*}\right)^{1/4} \cdot \exp\left\{-\frac{(x - X)^2}{2\alpha} + \frac{i}{\hbar}\left[(x - X)\,P + \theta\right]\right\} \tag{26}$$

Here $\alpha(t)$ and $\alpha^*(t)$ are the complex dispersion and its conjugate and $\theta(t)$ is a real phase. Moreover, $X(t) = \langle x \rangle$ and $P(t) = \langle p \rangle = \langle -i\hbar \frac{\partial}{\partial x} \rangle$. For this wave function the explicit form of W is

$$W = \gamma(x - X)P + \frac{i\hbar}{4}\gamma(x - X)^2 \left(\frac{1}{\alpha} - \frac{1}{\alpha^*}\right) \quad . \tag{27}$$

The first moments are known[26] to yield the correct Ehrenfest limit

$$\dot{X} = P/M \tag{28a}$$

$$\dot{P} = -K(X - X_o) - \gamma P \tag{28b}$$

The time evolution of α and θ is governed by

$$i\dot{\alpha} = -\frac{\hbar^2}{m} + K\alpha^2 - \frac{i\hbar}{2}\gamma\frac{\alpha}{\alpha^*}(\alpha - \alpha^*) \tag{29a}$$

$$\dot{\theta} = \frac{\hbar^2}{4m}\left(\frac{1}{\alpha} + \frac{1}{\alpha^*}\right) + L(X, P/M) \tag{29b}$$

where $L(X,\dot{X})$ is the classical Lagrangian.

We also need to study to evolution of the second moments

$$\chi = \langle x^2 \rangle - X^2 = \frac{1}{2}(\mathrm{Re}\ \alpha^{-1})^{-1} \tag{30a}$$

$$\phi = \langle p^2 \rangle - P^2 = \frac{\hbar^2}{2}(\mathrm{Re}\ \alpha)^{-1} \tag{30b}$$

$$\sigma = \langle \frac{1}{2}(xp + px) \rangle - XP = \frac{\hbar}{2} \frac{\mathrm{Im}\alpha}{\mathrm{Re}\alpha} \tag{30c}$$

The equations of motion for these quantities are[26,27])

$$\dot{\chi} = 2\sigma/M \tag{31a}$$

$$\dot{\phi} = -2K\sigma - 2\gamma\phi + \frac{\hbar^2\gamma}{2\chi} \tag{31b}$$

$$\dot{\sigma} = -K\chi + \phi/M - \gamma\sigma \tag{31c}$$

We note that the relation $\chi\phi - \sigma^2 = \hbar^2/4$ remains true at all times.

It is an important feature of the adopted description that when the quantities M, K, X_o and γ depend slowly on time an arbitrary gaussian wave function will evolve towards the time-dependent ground state of the oscillator, i.e., towards that gaussian which is characterized by the instantaneous values of M, K, and X_o. In particular, when there is no time dependence of M, K, and X_o the gaussian decays towards the ground state. This property of eq. (24) is distinct from other frictional Schrödinger equations proposed in the literature.

The above dynamical equations for the second moments are identical to those provided by the quantal master equation derived from linear response theory[3,4,30]) and by zero-temperature time-dependent perturbation theory[31]). However, the present case is more general in that it allows a time dependence of the various coefficients.

The diffusion coefficient for the energy change is given by

$$D(t) = \frac{\hbar^2 \gamma(t)}{4m(t)\ \chi(t)} \tag{32}$$

and the rate of energy change, equal to the drift coefficient, is

$$\dot{E} = \frac{d}{dt}\ \langle H_o \rangle = -\left(\gamma + \frac{\dot{M}}{M}\right)(P^2 + \phi)/M + D \tag{33}$$

When the harmonic oscillator is time independent the ground-state dispersion is given by $\chi_{gs} = \hbar/(2M\Omega)$ and we obtain the zero-temperature limit of the fluctuation-dissipation theorem[31]),

$$D = \frac{\hbar}{2}\ \gamma M\Omega \tag{34}$$

We wish to emphasize that (1) the present treatment does not rely on a pertubation-like approach and (2) it allows a non-adiabatic time dependence of the dynamical coefficients to be introduced in a natural way. Consequently, there is no need to discuss the characteristic time scales of the collective mode and the loss mechanism.

4. Calculated results

We have carried out dynamical calculations with the model described above for cases of experimental interest. The general features of the charge-asymmetry dynamics are illustrated in figs. 3 and 4.

In fig. 3 the time evolution of the mean projectile charge number $\langle Z \rangle$ has been plotted for a number of different angular momenta L. The case considered is 430 MeV ^{80}Kr on ^{92}Mo for which experimental data exist[6]). For large angular momenta (or impact parameters) the neck between the two nuclei remains rather constricted and the corresponding inertia and damping coefficients are rather large. Consequently the flow through the neck is inhibited and motion in the charge-asymmetry degree of freedom is overdamped. The equilibrium value of $\langle Z \rangle$ is then approached in a slow, monotonic fashion; for the highest angular momenta this motion is truncated by the pinch-off of the neck before the equilibrium value is reached. This overdamped character of the mode gradually changes as the collisions become more central. The nuclei then approach each other more closely and the neck becomes wider. The corresponding inertia and damping coefficients are in turn smaller and the flow may proceed more freely. An underdamped, oscillatory convergence toward the equilibrium value results. For each impact parameter (and corresponding angular momentum) the value of $\langle Z \rangle$ is fixed when the neck between the fragments closes. This point is indicated by a large dot on the

curve. Extending these lines to larger times we have constructed (along the righthand side of the figure) a curve for the final observed value of $\langle Z \rangle$ as a function of angular momentum. The trajectory calculations on which these curves are based can be used to establish a connection between angular momentum L and energy loss E* so the different calculated values of $\langle Z \rangle$ can be compared with experiment. Note that $\langle Z \rangle$ overshoots its equilibrium value during some of the small impact parameter collisions. However, this motion is damped out by the end of the reaction so that no overshoot appears in the final value. Perhaps some combination of target, projectile and bombarding energy can be found that would result in the prediction of an observable overshoot.

In fig. 4 we display the dynamical evolution of the full-width at half-maximum $\Gamma_{FWHM} = 2.355 \sqrt{\chi}$ where χ is defined by eq. (30a). The change from overdamped to underdamped motion is also reflected in this figure; for high L-values a monotonous growth of Γ occurs while for low L-values an oscillatory behavior is apparent. The frequency associated with the width oscillations is twice as large as that of the average value, due to the harmonic character of the motion. For the lower values of the angular momentum the charge asymmetry mode approaches its equilibrium distribution while there is still good communication between the two binary partners. From here on, as the neck grows longer during the outward radial motion, the distribution adjusts adiabatically to the instantaneous equilibrium value. Since the inertia is growing during

this phase, the corresponding equilibrium width is shrinking. This is clearly seen in the figure. Prior to the final snapping, the motion of the neck radius is accelerated and the corresponding variation in the inertia becomes so rapid that the wave function can no longer adjust adiabatically. During this stage the character of the motion changes from adiabatic to sudden and a "freeze-out" occurs after which the width remains constant. If it were not for this the non-adiabatic freeze-out the final width would have shrunk to zero as is appropriate for a vanishing neck radius. The actual value attained by the width depends on the details of the final stages of the neck dynamics.

The inclusion of the damping is an essential part of our dynamical description of the charge asymmetry. As it turns out, the value of the friction coefficient γ determined from the Giant Dipole Resonance width produces smooth curves for $\langle Z \rangle$ and Γ as a function of the energy loss E*. The calculated results are rather stable with respect to a variation of γ, but if it is increased by more than a factor of five the evolution toward equilibrium would begin to be somewhat slower than is indicated by experiment. On the other hand, if γ is reduced by more than a factor of five the calculated results for $\langle Z \rangle$ and Γ would begin to exhibit observable oscillations as a function of E*. An example of such overshoot behavior can be seen in refs. [7,8]) where a time-independent damping coefficient has been used.

In fig. 5 the calculated results are compared with the experimental data of ref. [6]). The upper portion of the figure

shows the mean charge ⟨Z⟩ and the lower portion shows the width Γ of the final charge distribution at a fixed mass partition; both quantities are plotted as functions of the total center-of-mass kinetic energy loss E* which is approximately the same as the induced intrinsic excitation in the fragments.

The primary experimental data are shown as the open dots on the upper portion of the figure and the dashed curve results after correction for neutron evaporation has been made [6]). No error bars are show in ref. [6]) but the fact that the resulting dashed curve does not go through Z = 36 at E* = 0 indicates that the errors must be fairly large. The solid curve represents the results displayed in figs. 3. Due to the restricted shape parametrization (two undeformable spheres joined by a cylindrical neck) the total obtainable energy loss is limited to about 50 MeV in the dynamical trajectory calculations. Up to this value, however, the calculations agree fairly well with the measured values. The slope is nearly the same and the vertical shift is within the error of half a change unit quoted in ref. [6]).

The error bars for the measured Γ values appearing in the present figure are those given in refs. [7,8]). They are fairly large and the exact trend of the data is not easy to discern. The present calculations give a quick rise of Γ with E*, followed by a broad maximum. The maximum occurs at around E* = 35 MeV in agreement with the data but it is not as pronounced. The behavior at large energy losses can not be determined due to the mentioned limitations of the shape

parameterization. The overall magnitude of the calculated curve is seen to fall somewhat below the experimental data.

Figure 6, which is similar to fig. 5b, displays the calculated and measured values of Γ_{FWHM} for the case of 900 MeV ^{132}Xe on ^{197}Au which has also been studied experimentally [32]. The general dynamical features are similar to the illustrations in figs. 3 and 4 discussed above. In this case though, there is no visible drift in Z (at most 0.1 charge unit) which is to be expected since the system is already from the outset close to equilibrium with respect to charge asymmetry. The overall collision time is somewhat shorter than in the previous case. For example, for head-on collisions the interaction time is 20×10^{-22} sec rather than 30×10^{-22} sec. The error bars on the width Γ indicate the variation in Γ with the mass asymmetry of the system rather than experimental errors in any particular Γ-value [7,8]. The calculations are shown by the solid curve and the correspondence with the data is quite satisfactory. In this case oscillations in $\Gamma(E^*)$ do in fact occur but they are minute and hardly measurable.

5. Concluding remarks

In this paper we have embarked, rather brashly, on a collective, quantal description of the charge equilibration in damped nuclear collisions, in spite of the fact that this approach touches on nearly every fundamental question in macroscopic nuclear dynamics. The first fundamental question is whether or not it is even appropriate to treat the charge asymmetry as an elementary collective mode in the dinucleus. Alternatively, one could consider the change in charge asymmetry as resulting exclusively from the stochastic exchange of individual nucleons and describe the equilibration as a diffusion process governed by a master equation[33]). Both mechanisms are probably present but a proper framework for their simultaneous treatment has not yet been developed. A second fundamental question concerns the appropriateness of the hydrodynamic assumptions concerning the flow of neutrons and protons back and forth through the neck. Other important questions arise in connection with our assumption that all the coupling between the charge asymmetry mode and the other degrees of freedom of the system can be accounted for by means of a frictional Schrödinger equation with a time-dependent Hamiltonian; the time dependence of the stiffness and mass parameters describes the coupling to the other collective modes while the coupling to the intrinsic degrees of freedom is all hidden in the damping coefficient.

Nevertheless, by proceeding step by step along the program outlined in the introduction we have arrived at a number of results for comparison with experiment. We are encouraged by the fact that these predictions are consistent with the observations. This is especially significant since all the coefficients entering in the various formulas are either fundamental nuclear constants or have been otherwise fixed beforehand so that there are no adjustable parameters.

A treatment somewhat similar to ours can be found in the work of Gregoire, Hofmann, Ngô and others[7,8,30]) who undertake to provide a description of the charge equilibration process in terms of a quantal master equation. This reduces to an approach like ours since the internal excitation is small. They parameterize the duration of the collision and ignore the time dependence of the dynamical coefficients. An unexpectedly large variation in the energy of the charge asymmetry mode from case to case results when the coefficients in the theory are adjusted so as to reproduce observation.

The treatment of the charge asymmetry mode as a manifestation of the Giant Dipole Resonance in a dumbbell shaped dinuclear complex is a step toward opening up new region of study. Heretofore giant resonances of different multipolarity and isospin have usually been considered only for spherical (or slightly deformed) nuclei. (For a notable exception see ref.[34])). What we have begun to see here is that our understanding of processes like fission and heavy ion reactions may be broadened by considering the behavior of giant resonances in the corresponding highly deformed shapes.

Acknowledgements

The authors have benefited from discussions with W. J. Swiatecki throughout the course of this work. They also wish to acknowledge conversations with G. Mantzouranis during the early stages of the project.

Two of us (E.S.H. and B.R.) wish to thank the members of the Nuclear Theory Group at the Lawrence Berkeley Laboratory for their warm hospitality. One of us (E.S.H.) is grateful to the Consejo Nacional de Investigaciones Cientificas y Tecnicas, Argentina for financial support. Another of us (B.R.) is indebted to the Direction des Affaires Scientifiques, Ministère des Affaires Etrangères, France, for financial support.

Table 1.

Typical values of the frequency Ω, mass M, stiffness K, energy $\hbar\Omega$, and friction coefficient γ for the two dinuclear systems considered; the values correspond to the point of largest neck opening along the head-on trajectories.

	Ω ($dsec^{-1}$)[a]	M (MeV $dsec^2$)	K (MeV)	$\hbar\Omega$ (MeV)	γ ($dsec^{-1}$)
$^{86}Kr + ^{92}Mo$	0.88	5.21	4.03	5.79	0.37
$^{132}Xe + ^{193}Au$	0.74	4.48	2.48	4.90	0.38

a) 1 dsec=10^{-22} sec.

References

1) H. Steinwedel and J. H. Jensen, Z. Naturforsch. 52 (1950) 413

2) P. Fong, "Statistical Theory of Nuclear Fission," Gordon and Breach, New York (1969)

3) D. L. Hill and J. A. Wheeler, Phys. Rev. 89 (1953) 1102

4) W. J. Swiatecki and H. M. Blann, unpublished notes (1961); W. J. Swiatecki, lecture at Princeton University, 7 March 1961

5) L. G. Moretto, J. Sventek and G. Mantzouranis, Phys. Rev. Lett. 42 (1979) 563

6) M. Berlanger, A. Gobbi, F. Hanappe, U. Lynen, C. Ngô, A. Olmi, H. Sann, H. Stelzer, H. Richel, and M. F. Rivet, Proc. Int. Workshop on Gross Properties of Nuclei and Nuclear Excitations VII, Hirschegg, Austria, Jan. 1979; also Z. Phys. A291 (1979) 133

7) C. Grégoire, R. Lucus, C. Ngô and H. Hoffmann, Proc. IVth Balaton Conf. on Nucl. Phys., Keszthely, Hungary, June 1979

8) H. Hofmann, C. Grégoire, R. Lucas and C. Ngô, preprint DPh-N/MF/79/22, CEN, Saclay, July 1979

9) H. Nifenecker, J. Blachot, J. P. Bocquet, R. Brissot, J. Crancon, C. Hamelin, G. Mariolopoulos and Ch. Ristori, preprint Centre d'Etudes Nucleaires, Grenoble, July 1979

10) J. Randrup, Nucl. Phys. A307 (1978) 319

11) J. Randrup, work in progress

12) J. Błocki, J. Randrup, W. J. Swiatecki and C. F. Tsang, Ann. Phys. (NY) 105 (1977) 427-462

13) W. D. Myers, Nucl. Phys. A204 (1973) 465

14) W. D. Myers and W. J. Swiatecki, Ark. Fys. 36 (1967) 343

15) W. J. Swiatecki, lectures presented at the Intern. School of Nuclear Physics, "Ettore Majorana," Center for Scientific Culture, Erice-Trapani, Sicily, March 1979; Lawrence Berkeley Laboratory preprint LBL-8960

16) J. Błocki, Y. Boneh, J. R. Nix, J. Randrup, M. Robel, A. J. Sierk and W. J. Swiatecki, Ann. Phys. (NY) 113 (1978) 330-386

17) S. E. Koonin and J. Randrup, Nucl. Phys. A289 (1977) 475-510

18) J. Randrup, Ann. Phys. (NY) 112 (1978) 356-365

19) C. T. Alonso, Proc. Intern. Coll. on Drops and Bubbles, Calif. Inst. of Tech. and JPL. August, 1974, p. 139

20) W. D. Myers, "Droplet Model of Atomic Nuclei," IFI/Plenum, New York (1977)

21) W. D. Myers, W. J. Swiatecki, T. Kodama, L. J. El-Jaick and E. R. Hilf. Phys. Rev. C15 (1977) 2032-2043

22) G. E. Brown, J. S. Dehesa and J. Speth, preprint, August 1979

23) H. Lamb, "Hydrodynamics," Treatise on the Mathematical Theory of the Motion of Fluids, 1879, sixth edition titled "Hydrodynamics," Dover, 1945

24) U. Brosa and H. J. Krappe, Z. Physik A284 (1978) 65-69

25) R. W. Hasse and P. Nerud, J. Phys. G2 (1976) L101

26) R. W. Hasse, J. Math. Phys. 16 (1975) 2005

27) B. Remaud and E. S. Hernandez, Lawrence Berkeley Laboratory report LBL-9506, 1979, to be published

28) M. D. Kostin, J. Stat. Phys. 12 (1975) 145

29) K. K. Kan and J. J. Griffin, Phys. Lett. 50B (1974) 241

30) H. Hofmann, A. S. Jensen, C. Ngô, P. J. Siemens, IVth Balaton Conf. on Nuclear Physics, Keszthely, Hungary (1979), to be published

31) R. W. Hasse, Nucl. Phys. A318 (1979) 480

32) G. Wirth, W. Brüchle, H. Gäggeler, J. V. Kratz, M. Schadel, I. Warnecke, G. Hermann, M. Weis, R. Lucas and J. Peitov, Proc. Intern. Workshop on Gross Properties of Nuclei and Nuclear Excitations VII, Hirschegg, Austria, Jan. 1979, INKA-Conf.-79-001-003

33) J. Randrup, "Transport of charge and mass in nuclear collisions," NORDITA preprint (1978)

34) W. E. Updegraff and D. S. Onley, Nucl. Phys. A161 (1971) 191

Figure Captions

Fig. 1. The geometrical quantities used to describe the dinuclear complex during the collision.

Fig. 2. Typical results from the trajectory calculations for the time evolution of the neck parameters and the intertial mass associated with the charge asymmetry mode.

Fig. 3. The time evolution of the mean change $\langle Z \rangle$ for a number of different initial angular momenta L. The point of neck closure is indicated on each curve by the solid dot.

Fig. 4. The time evolution of the charge width Γ_{FWHM} for a number of different initial angular momenta L; similar to fig. 3.

Fig. 5. Measured and calculated values of the mean charge $\langle Z \rangle$ and charge dispersion Γ_{FWHM} (for the projectile-like fragment) as a function of energy loss in the reaction 430 MeV ^{86}Xe on ^{197}Au.

Fig. 6. Measured and calculated values of the charge dispersion Γ_{FWHM} as a function of energy loss E* in the reaction 900 MeV ^{132}Xe on ^{197}Au.

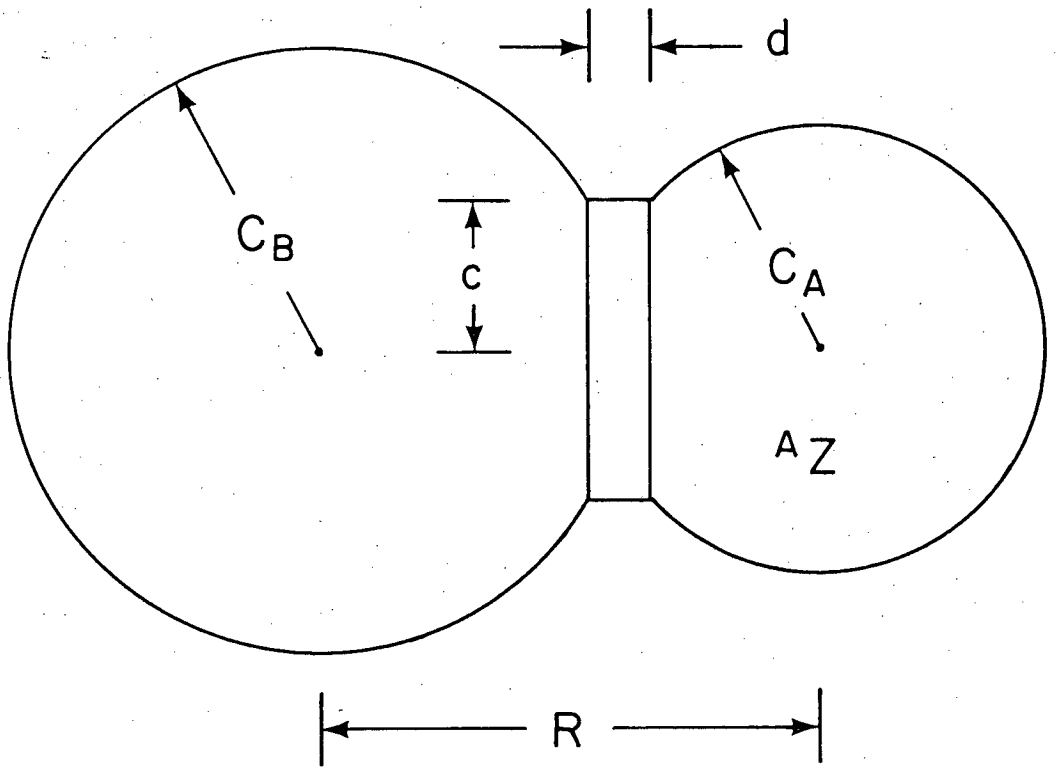

XBL 799-2951

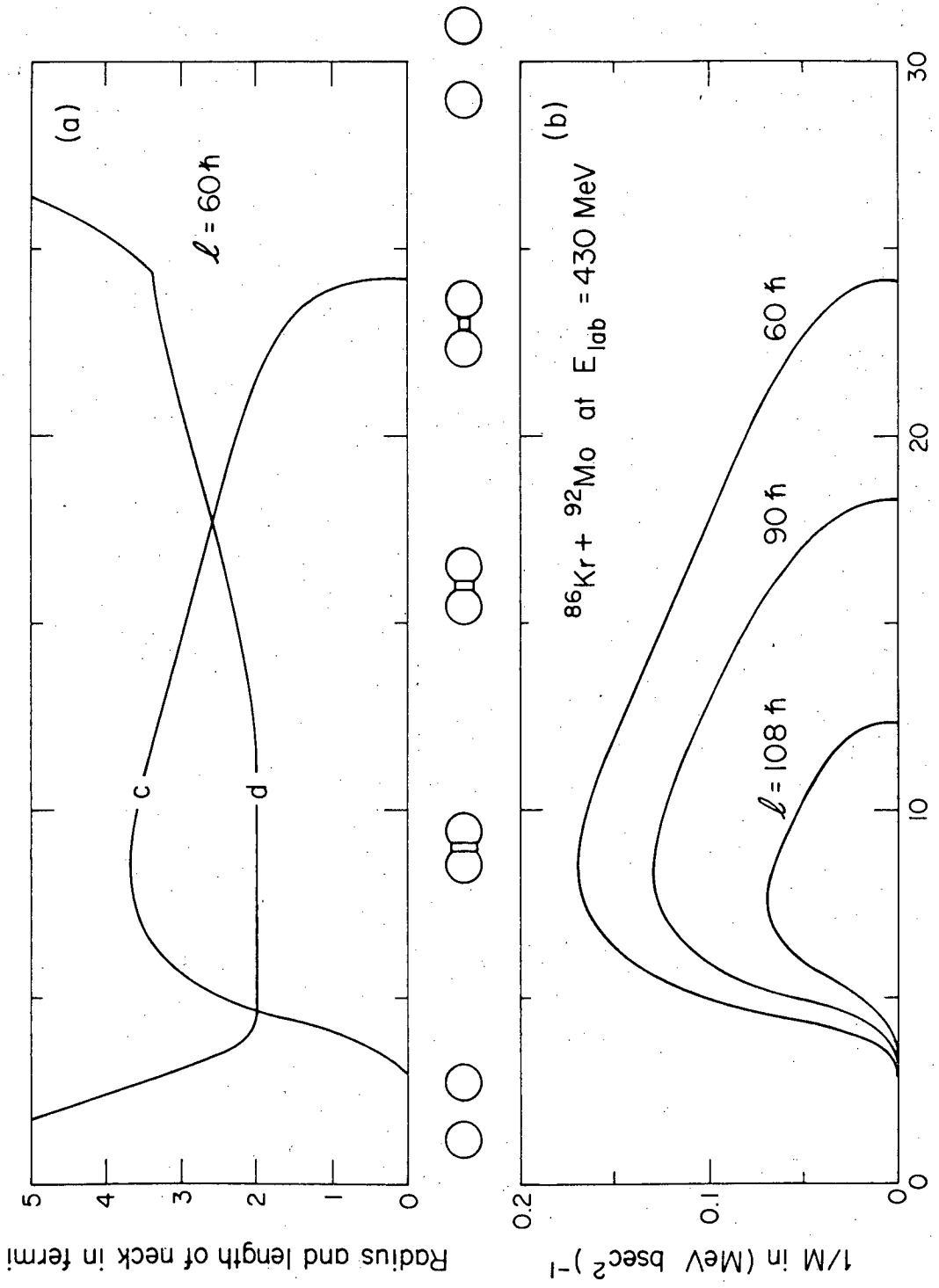
(a)
ℓ = 60 ħ
c
d
Radius and length of neck in fermi
(b)
$^{86}Kr + ^{92}Mo$ at E_{lab} = 430 MeV
ℓ = 108 ħ
90 ħ
60 ħ
1/M in (MeV bsec^2)$^{-1}$
Time in 10^{-22} sec

XBL799-2953

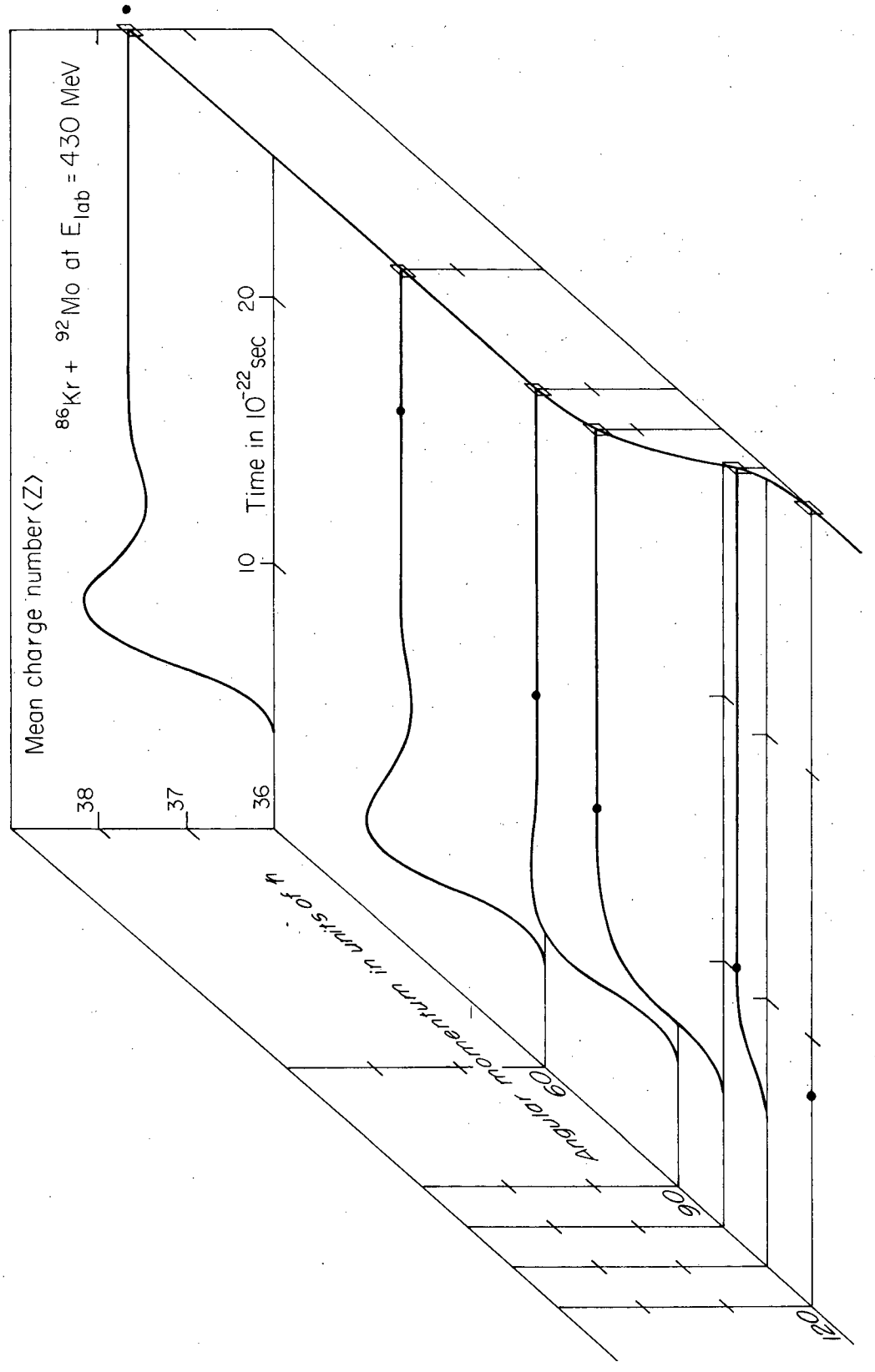
Mean charge number ⟨Z⟩
$^{86}Kr + {}^{92}Mo$ at $E_{lab} = 430$ MeV
Time in 10^{-22} sec
10
20
36
37
38
Angular momentum in units of ħ
60
90
120

XBL 799-2956

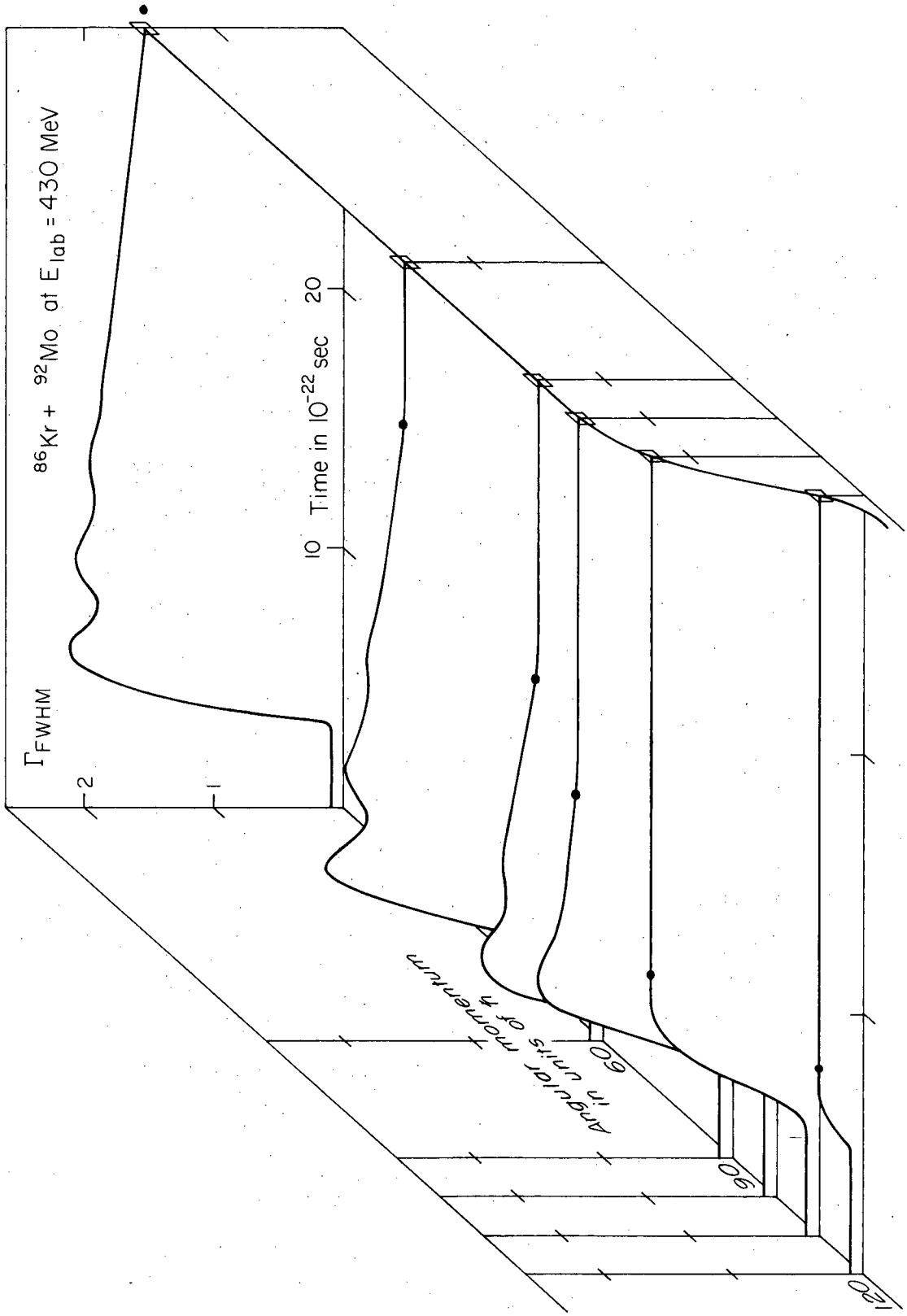
$^{86}Kr + ^{92}Mo$ at $E_{lab} = 430$ MeV
Γ_{FWHM}
2
1
10 Time in 10^{-22} sec 20
Angular momentum in units of ħ
60
90
120

XBL 799-2955

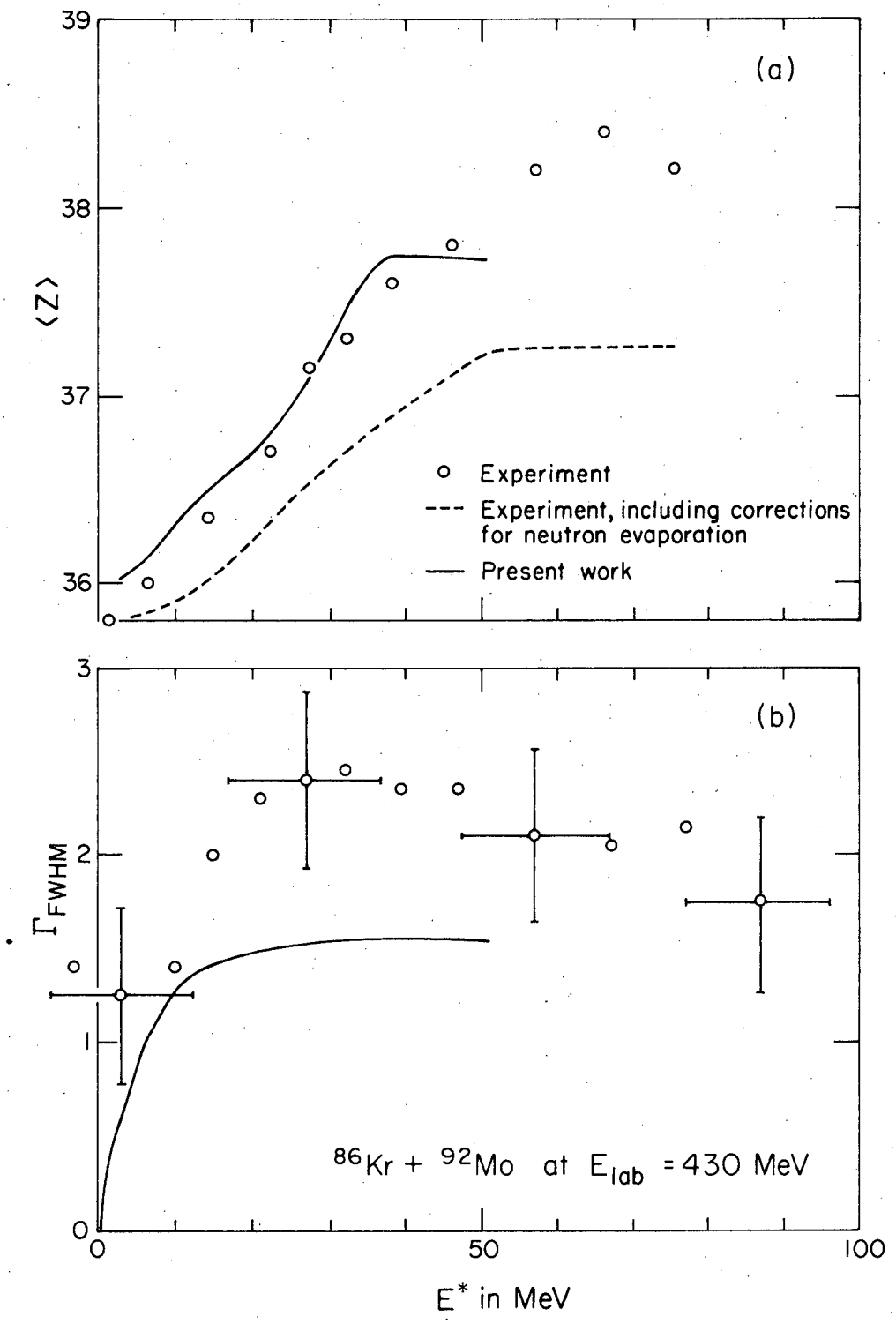
(a)
39
38
37
36
⟨Z⟩
Experiment
Experiment, including corrections for neutron evaporation
Present work
(b)
3
2
1
0
Γ_{FWHM}
$^{86}Kr + ^{92}Mo$ at E_{lab} = 430 MeV
0
50
100
E* in MeV

XBL 799-2954

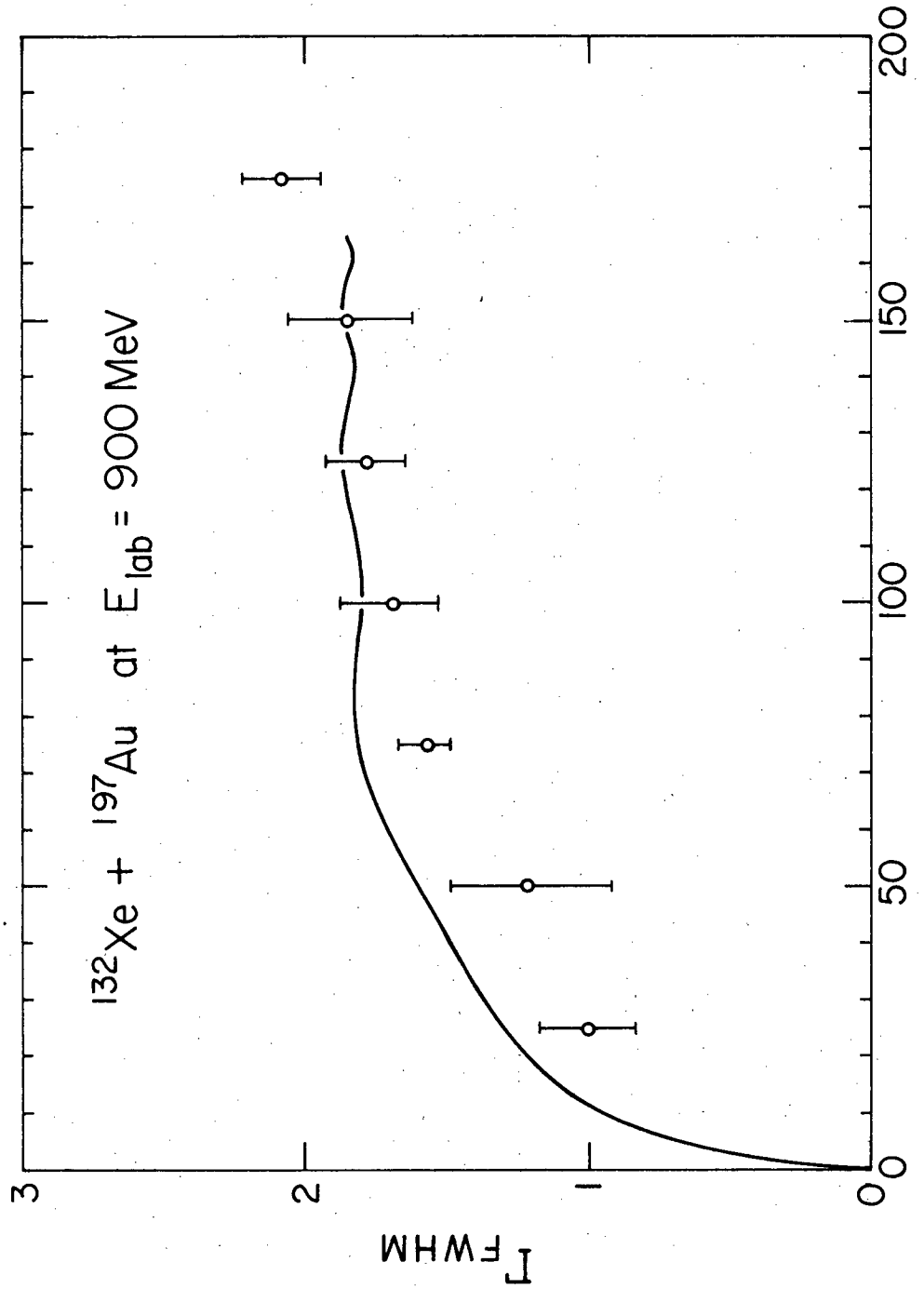
$^{132}Xe + ^{197}Au$ at $E_{lab} = 900$ MeV
Γ_{FWHM}
E^* in MeV
0
1
2
3
0
50
100
150
200

XBL799-2952

TECHNICAL INFORMATION DEPARTMENT
LAWRENCE BERKELEY LABORATORY
UNIVERSITY OF CALIFORNIA
BERKELEY, CALIFORNIA 94720